The Ground Motion Excited by the Olyutorskii Earthquake of April 20, 2006 and by Its Aftershocks Based on Digital Recordings

O. S. Chubarova[a], A. A. Gusev[a], and V. N. Chebrov[b]

[a] Institute of Volcanology and Seismology, Far East Division, Russian Academy of Sciences,
Petropavlovsk-Kamchatskii, 683006 Russia
[b] Kamchatka Branch, Geophysical Service, Russian Academy of Sciences, Petropavlovsk-Kamchatskii, 683006 Russia
Received June 10, 2008

Abstract—We studied broadband digital records of the $M_W = 7.6$ Olyutorskii earthquake of April 20, 2006 and its aftershocks at local and regional distances. We have made a detailed analysis of data on peak ground motion velocities and accelerations due to aftershocks based on records of two digital seismic stations, Tilichiki (TLC) and Kamenskoe (KAM). The first step in this analysis was to find the station correction for soil effects at TLC station using coda spectra. The correction was applied to the data to convert them to the reference bedrock beneath the Kamenskoe station. The second step involved multiple linear regression to derive mean relations of peak amplitude to local magnitude ML and distance R for the Koryak Upland conditions. The data scatter about the mean relations is comparatively low (0.22–0.25 log units). The acceleration amplitudes for $M_L = 5$, $R = 25$ km are lower by factors of 2–3 compared with eastern Kamchatka, the western US, or Japan. A likely cause of this anomaly could be lower stress drops for the aftershocks.

INTRODUCTION

The large ($M_W = 7.6$) shallow Olyutorskii earthquake of April 20(21), 2006 is the greatest event known to have occurred in the area of the Koryak Autonomous Okrug (KAO). The level of shaking reached intensity VIII–IX in the epicentral zone. The ground motion records of the Olyutorskii earthquake are of great interest. No records of strong ground motion were made in the KAO area until May 2006. However, some limited information on the ground motion excited by the main shock can still be gathered from records of the KAM permanent digital broadband seismic station (DBBSS), which is operated in the village of Kamenskoe in the framework of Russian–Japanese scientific cooperation. The peak amplitudes at the BH* channels used at Kamenskoe were unfortunately too high for the main shock and even the larger aftershocks to be recorded without distortion.

Soon after the earthquake occurred, workers with the Kamchatka Branch (KB) of the Geophysical Service (GS) of the Russian Academy of Sciences (RAS) (E.P. Tokarev, V.N. Kozlov, and T.V. Shevchenko) installed a digital accelerometer at the village of Tilichiki in the epicentral zone in a troubled situation; this made it possible to record hundreds of aftershocks of the Olyutorskii earthquake without distortion. This material is of great interest.

The present study contains a preliminary analysis of digital ground motion records for the Olyutorskii earthquake. Apart from data recorded in the epicentral zone, we also used materials from other DBBSSs located as far as 100 km from the epicenter.

DIGITAL RECORDING OF GROUND MOTION IN KAMCHATKA AND IN THE KORYAK AUTONOMOUS OKRUG

Important and interesting seismological studies have been carried out in Kamchatka since 1962, with the main instrument being seismographs with galvanometric recording on photographic paper. In recent years nearly all records were made by a network of self-contained stations with analog FM–FM telemetry and digital storage. This observational system could not record strong ground motions. These could be recorded by a restricted number of accelerographs with direct optical recording and velocity meters based on the 5-second C4C pendulum. The most extensive recording of strong ground motion was in 1985–1988, when 11 recording stations were operated in the Petropavlovsk-Kamchatskii area, in addition to 18 stations outside the city limits. These instruments were operated in trigger mode with no accurate timing, while their reliability was always rather limited owing to several objective and subjective factors. We wish to explain at this point that one or two dozen sensitive seismographs installed in Kamchatka were sufficient to determine the hypocenters and energies of 1000 to 2000 small earthquakes occurring in the region each year, supplying data

Table 1. Parameters of digital seismic stations

Station	Station code	$\varphi°$, N	$\lambda°$, E	h, m	Soil	Sensor type	Recorder	Sampling rate, f_ω, s^{-1}	Opera-tion mode	Δ, km
Tilichiki	TLC	60.4302	166.0563	52	Gravel permafrost	CMG-5T(A)	GSR-24	100	Trigger mode	95
Kamenskoe	KAM	62.4560	166.2100	64	Bedrock	STS-1 (V)	Quanterra	20	Continuous	175
Nikol'skoe	BKI	55.1939	165.9835	10	Poorly coherent sandstone	CMG-5T(A)	GSR-24	100	Trigger mode	650
Krutoberegovo	KBG	56.2584	162.7127	18	Pyroclastic material	CMG-5T(A)	GSR-24	100	Continuous	590
Petropavlovsk	PET	53.0233	158.6501	102	Bedrock	STS-IV GS13 (V)	Quanterra	20, 80	Continuous	1030

Note: φ is latitude, λ longitude, Δ epicentral distance (from the instrumental mainshock epicenter). A or V mark channel type (accelerometer or velocity meter). CMG-5T denotes a forced-balance accelerometer, GSR-24 a digital seismic recorder, Quanterra is a digital seismic station with STS-1 and STS-IV sensors recording BH* and GS13 recording EH*.

for detailed studies of seismicity geography, earth structure, and so on. At the same time, strong motion instruments characterize ground motion at the installation site only, and it is hardly legitimate to extend the results to large areas. The sparse network of strong ground motion instruments in Kamchatka operated during the period 1962–2000 has accumulated extremely valuable, but rather fragmentary strong ground motion records [2]. Aftershock studies are therefore of great interest, because the material thus acquired is extensive, even though it is not always representative. It is also rather desirable to have digital recordings, which will make the observational system more advanced, both as regards convenience and automation of data processing on the one hand and expansion of the spectrum of recorded motion toward lower frequencies on the other.

This situation began to improve in 1993 as work started at the Petropavlovsk station (DBBSS PET) within the IRIS consortium framework. The station is able to record strong shocks via a low sensitivity channel based on a feedback accelerometer (FBA). The records of that station were used to start research on ground motions in Kamchatka based on direct digital records in a broad frequency range. However, it was only after 2002 that a network of digital instruments proper began to be installed (which is not yet finished). The Olyutorskii earthquake was a test for the capabilities of that network.

This study is based on records of several seismic stations and instruments; Table 1 provides a brief overview of these. We note that the broad dynamic range of modern digital seismic stations makes it possible to record both strong ground motion and small earthquakes using one and the same instrument.

Since the Olyutorskii earthquake occurred at an appreciable distance from the Kamchatka network, we studied the records of the stations in the Kamchatka network that were located nearest to the epicenter (BKI and

KBG), as well as the PET base station, not counting the KAM and TLC stations, which are situated in the KAO (Fig. 1). Calibration control was performed at the stations we used (except KAM) by comparing recordings of some channels and alternative digital channels for some selected earthquakes. The alternative channels were those at the MARS mobile station (Lennartz) for TLC (smaller events) and the C5C-OC feedback channels designed by the KB GS RAS (Yu.V. Shevchenko) for BKI and KBG and regional telemetry channels (PTCC) for PET. The MARS stations were as good as useless for strong ground motion study because of their insufficient dynamic range.

RAW DATA. PROCESSING PROCEDURES

This study is concerned with records of the Olyutorskii mainshock earthquake and aftershocks (Fig. 1, Table 2). The earthquake parameters listed in Table 2 were taken from the KB GS RAS catalog. The digital earthquake records were selected from the main digital archive available at the KB GS RAS. We investigated records in trace form, their Fourier spectra, and peak ground motion amplitudes. The peak amplitude data for the stations nearest to the epicentral zone (Tilichiki TLC and Kamenskoe KAM, 49 three-component records) were then used to find average relations of amplitude to magnitude and distance.

A new program package based on a previously developed technique [3] was used for data processing. The package makes partial use of the deconvolution module kindly lent by V.M. Pavlov. As regards the processing itself, the algorithm implements the following sequence of operations:

Selecting a segment to be processed (in dialog mode);

Correcting for the instrument's transfer function in the broadest range of frequencies possible by deconvolution "in the dark" in the frequency domain;
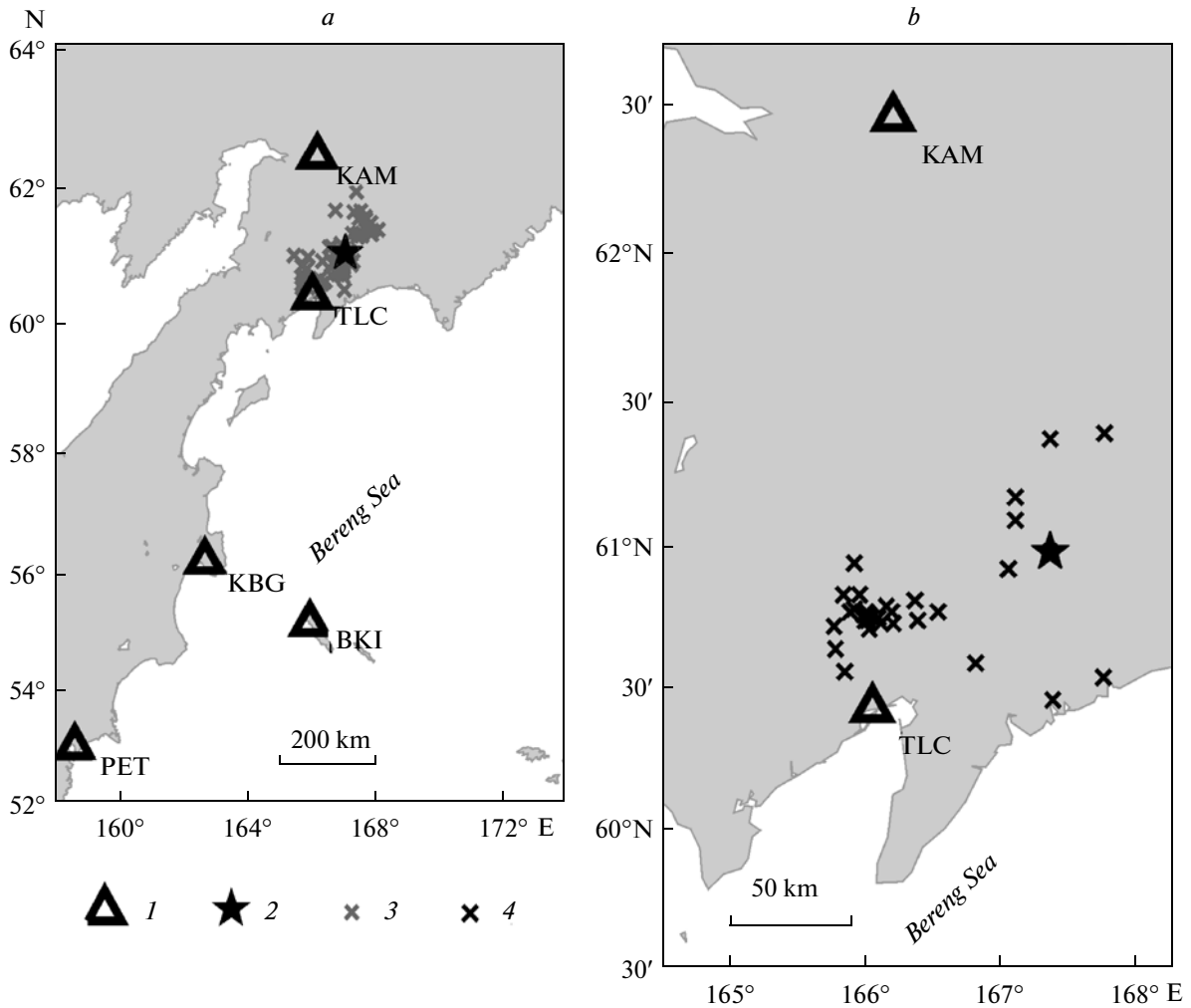
Fig. 1. Map of stations and earthquake epicenters: (*a*) rupture zone as outlined by the 3-day aftershocks, (*b*) aftershocks whose records have been used: (*1*) digital seismic stations, (*2*) mainshock epicenter, (*3*, *4*) aftershock epicenters.

Interactive selection of the working frequency band (lowest frequency f_1 and highest frequency f_2) for reliable recovery of signal amplitudes;

Repeated deconvolution in the frequency domain within the selected frequency band, calculating the recovered acceleration, velocity, and displacement;

Measuring the peak acceleration, velocity, and displacement;

Calculating a smoothed amplitude Fourier spectrum within the selected band with signal pre-whitening;

Calculating the response spectrum.

One important and essentially novel feature in the program package is the prewhitening procedure, which is used to find smoothed amplitude Fourier spectra. This method was originally developed for estimating the power spectra of stationary signals [1] and its first application was estimation of the smoothed Fourier spectrum of a seismic record. The method can strongly suppress distortions in spectral estimates when steep decreases or increases in the

spectrum occur. It is known that simple smoothing when used in such cases produces appreciable distortion in the estimates owing to power leakage from the "heavier" to the "lighter" portion of the smoothing window. This difficulty is a real one. In particular, an observed signal necessarily involves a steep (like the exponent $e^{-\kappa f}$) decay in the Fourier spectrum in the region of higher frequencies due to seismic wave attenuation in the earth. Also, body-wave acceleration spectra show steep decays in the region of lower frequencies (below the corner frequency). In both of these cases the spectra are sure to suffer distortion when ordinary smoothing is used. Prewhitening suppresses nearly all of the distortion.

The deconvolution and signal recovery procedure uses the parameters of the recovery frequency band (f_1, f_2). The value of f_2 was chosen as 0.6–0.7 of the Nyquist frequency $f_H = 0.5/\Delta t$, where Δt is the digitization step, while the value of f_1 was chosen so as to reduce the parasitic low frequency signal [3]. The choice of these parameters also

Table 2. List of earthquakes used in this study

Date	Time, h:min:s	$\varphi°$, N	$\lambda°$, E	H, km	K_S	M_L	m_b	Processed records were made at stations
April 20, 2006	23:24:57	60.98	167.37	1	15.7*	7.1	6.8	KAM KBG BKI PET
April 21, 2006	00:51:08	61.09	167.11	1	12.2	5.4	5.3	KAM
April 21, 2006	04:32:45	60.56	165.85	22	12.7	5.6	6.3	BKI KAM
April 21, 2006	11:14:12	61.39	167.77	0	13.5	6.0	5.8	BKI KAM
April 21, 2006	20:50:01	60.92	167.06	0	11.9	5.2	5.3	BKI KAM
April 22, 2006	07:21:58	61.17	167.11	14	12.6	5.6	5.8	BKI KAM
April 22, 2006	09:20:47	60.64	165.78	17	9.5	4.0	4.5	KAM
April 29, 2006	12:57:54	60.94	165.92	4	12.0	5.3	5.1	KAM
April 29, 2006	16:58:05	60.54	167.76	0	14.4	6.5	6.4	BKI KAM
May 7, 2006	00:54:54	60.46	167.39	0	10.0	4.3	4.6	TLC KAM
May 9, 2006	03:31:38	60.83	165.84	9	10.2	4.4	4.5	TLC KAM
May 9, 2006	11:02:20	60.74	166.02	5	13.0	5.8	5.6	TLC KAM BKI
May 11, 2006	12:50:09	60.83	165.96	6	9.6	4.1	4.6	TLC KAM
May 11, 2006	13:41:56	60.76	166.03	1	9.7	4.1	4.6	TLC KAM
May 14, 2006	05:16:47	60.74	166.00	10	10.7	4.6	4.7	TLC KAM
May 18, 2006	19:30:23	60.75	166.05	2	10.9	4.7	5.1	TLC KAM
May 22, 2006	11:11:56	60.75	166.10	3	14.2	6.4	6.0	TLC KBG BKI PET KAM
May 22, 2006	11:29:52	60.73	166.21	5	11.1	4.8	4.8	TLC KAM
May 22, 2006	11:43:51	60.81	166.37	10	10.5	4.5	4.6	TLC KAM
May 22, 2006	11:50:30	60.76	166.01	9	11.8	5.2	4.9	TLC KAM
May 22, 2006	12:04:49	60.77	166.20	5	11.6	5.1	4.9	TLC KAM
May 22, 2006	12:30:11	60.77	166.01	14	11.2	4.9	5.0	TLC KAM
May 22, 2006	13:03:08	60.73	166.12	12	12.6	5.6	5.3	TLC KAM
May 22, 2006	15:16:27	60.79	166.16	7	10.5	4.5	4.5	TLC KAM
May 22, 2006	22:40:42	60.74	166.39	6	10.3	4.4	4.5	TLC KAM
May 24, 2006	15:44:49	60.78	165.92	8	11.8	5.2	5.1	TLC KAM
May 24, 2006	20:48:44	60.71	166.03	15	10.7	4.6	5.1	TLC KAM
May 27, 2006	04:09:01	60.77	165.89	7	10.8	4.7	4.8	TLC KAM
May 27, 2006	23:57:52	60.76	165.99	17	10.8	4.7	4.5	TLC KAM
May 29, 2006	19:39:35	60.72	165.77	10	10.2	4.4	4.6	TLC KAM
June 9, 2006	07:25:17	60.59	166.82	32	10.0	4.3	4.6	TLC
July 7, 2006	11:56:04	60.77	166.54	29	10.0	4.3	4.3	TLC
August 11, 2006	06:45:42	61.37	167.37	6	10.2	4.4	4.7	TLC

Note: φ is latitude, λ longitude, H depth of focus, K_S energy class based on S waves, * denotes energy class K_c based on coda waves, $M_L = K_S/2 - 0.75$ is local magnitude, m_b body-wave magnitude.

partially affects the recovery result. In particular, records of the KAM velocity meters with $\Delta t = 0.05$ s cannot be used to recover that segment of the acceleration spectrum between 6–7 and 15 Hz. Similarly, accelerograms are not sufficient to recover the spectrum in the range 0.01–0.1 Hz. For this reason we used the following parameters for the velocity meters (BH* channels): $f_1 = 0.02$–0.03 Hz, $f_2 = 6$–7 Hz, the values for the accelerometers being $f_1 = 0.07$–0.1 Hz and $f_2 = 40$ Hz.

RESULTS OF DIGITAL RECORDING

The present section describes the processing and a first analysis of the records studied. We show graphic materials for the main shock and several larger aftershocks. The reconstructed ground motion signals (for acceleration, velocity, and displacement) are given for all three components, in addition to smoothed amplitude Fourier spectra for acceleration signals. Fourier spectra were invariably smoothed with a logarithmically constant window width,

about 0.1 decades (1/3 of an octave). More extensive graphic materials, including sample response spectra and tables of peak ground motion amplitudes, can be found in [6].

Figure 2 shows reconstructed ground motions for the main shock recorded at four stations. The distorted unprocessed velocity record at the KAM station at an epicentral distance of 175 km (Fig. 2e) illustrates the performance of the digital channel under overloaded conditions. The P-wave portion of about 15 s length was nevertheless recorded without distortion and examined later, see Figs. 2a–2d. We show acceleration (b), velocity (c), and displacement (d) traces, as well as smoothed acceleration Fourier spectra (a) for the three components. It can be seen that the spectrum is in the frequency band that is typical of such earthquakes (approximately between 0.4 and 7 Hz), but the upper spectral frequency may have been underestimated due to the use of the bandpass filter. Note that when the portion to be processed is selected by a window, as in the present case in which the oscillation range is increasing, the procedure leads to inevitable distortions in the region of lower frequencies. Actually, the P-wave signal was certain to have higher spectral amplitudes at frequencies below 0.2–0.3 Hz, and, therefore, higher velocity and displacement amplitudes. It can be asserted, however, that the acceleration signal was comparatively reliably reconstructed in the band below 6–7 Hz.

The other records shown were made at regional distances. For a good record made at the KBG station we show ground motion accelerations, velocities, and displacements (Figs. 2f–2h). It can be seen that the relative contributions of P, S, and surface waves are comparable for the velocity record, while the contribution due to P waves is small in the displacement record, which is dominated by well-pronounced surface waves and long period S. Displacement records are also shown for PET and BKI (Figs. 2i, 2j). These are dominated by surface waves. (The record at the BKI station, which was operated in trigger mode, is incomplete because of a poor tuning of the time window in trigger recording mode during the time of the main shock.)

Figure 3 shows results from the processing of P-wave record segments (from the first onset to S onset) at KBG and BKI. We begin by comparing the records of KBG and BKI. The band of acceleration frequencies on both of these records is approximately 0.4–2 Hz. Attenuation made the upper cutoff frequency much lower compared with the KAM spectrum. It is very interesting to note that the amplitude level at BKI is appreciably (by factors of 5–

10) lower compared with KBG, although their respective epicentral distances are not so very different (650 and 590 km). This difference is seen throughout the entire frequency band. It follows that a simple explanation of the observed differences by invoking differences in path attenuation is questionable, considering that the attenuation effects usually increase appreciably with frequency. Further P-wave propagation makes the spectral frequency band still narrower, as small as about 0.3–1 Hz at PET (at a distance of 1030 km).

Figure 4 shows processing results for the records of the 11:02 May 9, 2006 aftershock, which was recorded simultaneously at TLC and KAM. It is interesting to see an intensive onset of surface waves on the KAM displacement records. The Fourier spectral shapes both at TLC and KAM are rather ordinary and show some differences in this respect from those for the largest aftershock (May 22, 2006). One notes, however, that the high frequency decay in the TLC spectrum is relatively faster than for KAM, even though the epicentral distance for the latter station is shorter. Attenuation should have produced the opposite effect. The cause of this phenomenon seems to be the relative amplification of the 0.3–3 Hz band at TLC owing to site geology (see below).

A TECHNIQUE FOR STUDYING AMPLITUDE–DISTANCE–MAGNITUDE RELATIONS

We studied the peak amplitude vs. hypocentral distance vs. magnitude relations using 49 aftershock records (magnitude 4 or greater); these were mostly recorded by both TLC and KAM, or occasionally by only one of those two stations. Hypocentral distances were found from the S-P difference using I.P. Kuzin's travel–time table [8] assuming a depth of 10 km. The arrival times of the P and S waves were as reported by the KB GS RAS. This method for hypocentral distance estimation is sufficiently reliable and is sure to be free from potential hypocentral inaccuracies due to poor network geometry in the area of study. The present analysis of the amplitude–distance–magnitude relations is based on the local short-period M_L magnitude scale of the Kamchatka network as the basis; magnitudes in this scale are converted in a straightforward manner from the Fedotov energy class $K_S = K_{S1,2}^{\Phi 68}$ [10]. The conversion relies on the following considerations. It is customary to base the local magnitude on the log trace amplitude. Since the scale is defined as

$$K_S = 2\log(A_S/T_S) + f(r), \quad (1)$$

Fig. 2. Records of the April 20, 2006 main event at KBG, BKI, PET, and KAM: (a) Fourier acceleration spectrum based on the first 15 s of P-wave record at KAM, (b–d) (recovered) ground motion acceleration, velocity, and displacement for the first 15 s of P-wave record at KAM, (e) full original velocity meter record at KAM, (d–h) (recovered) ground motion acceleration, velocity, and displacement at KBG, (k) ground motion displacement at BKI and PET, the BKI record is incomplete. The peak values are marked by circles from here on.
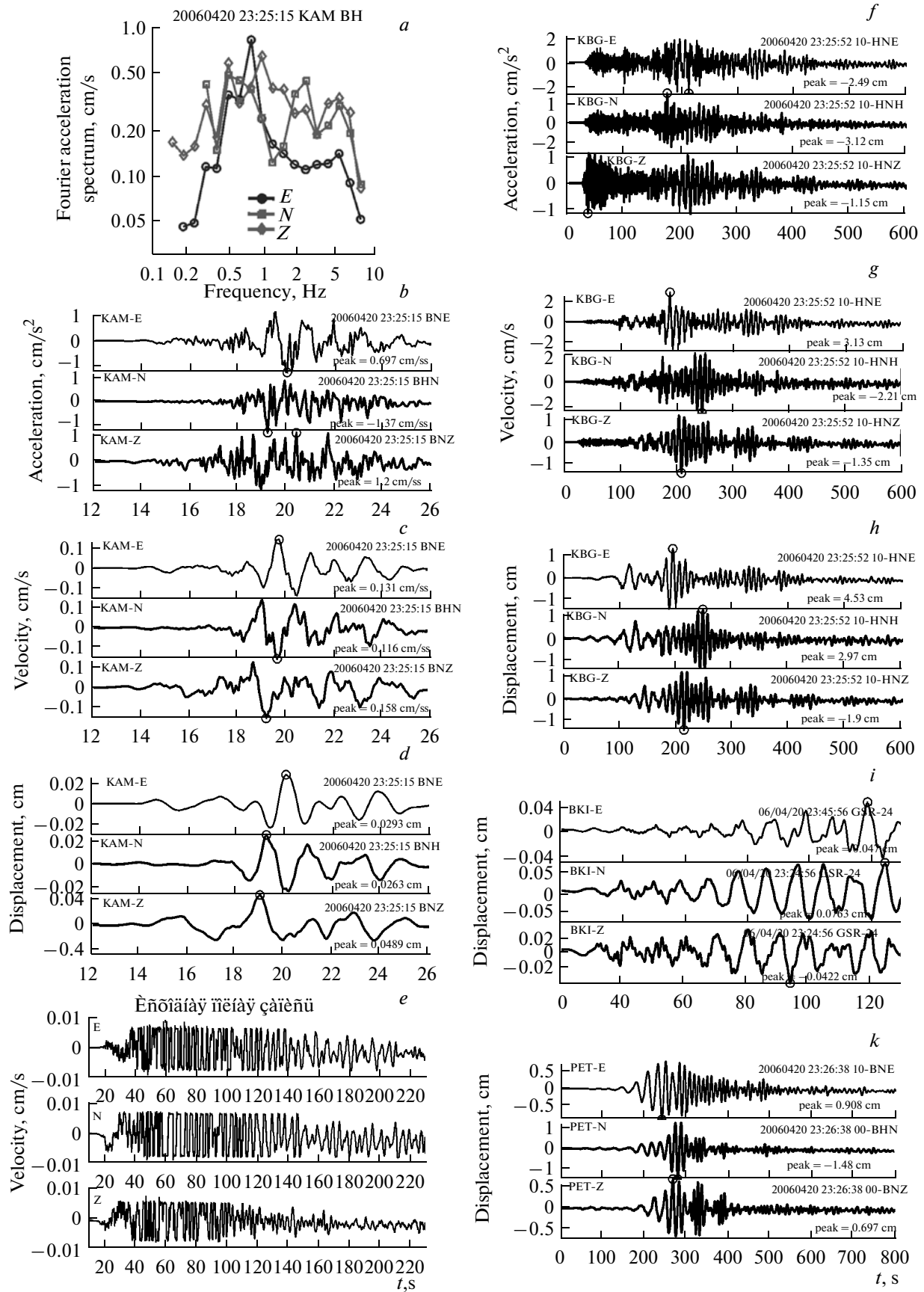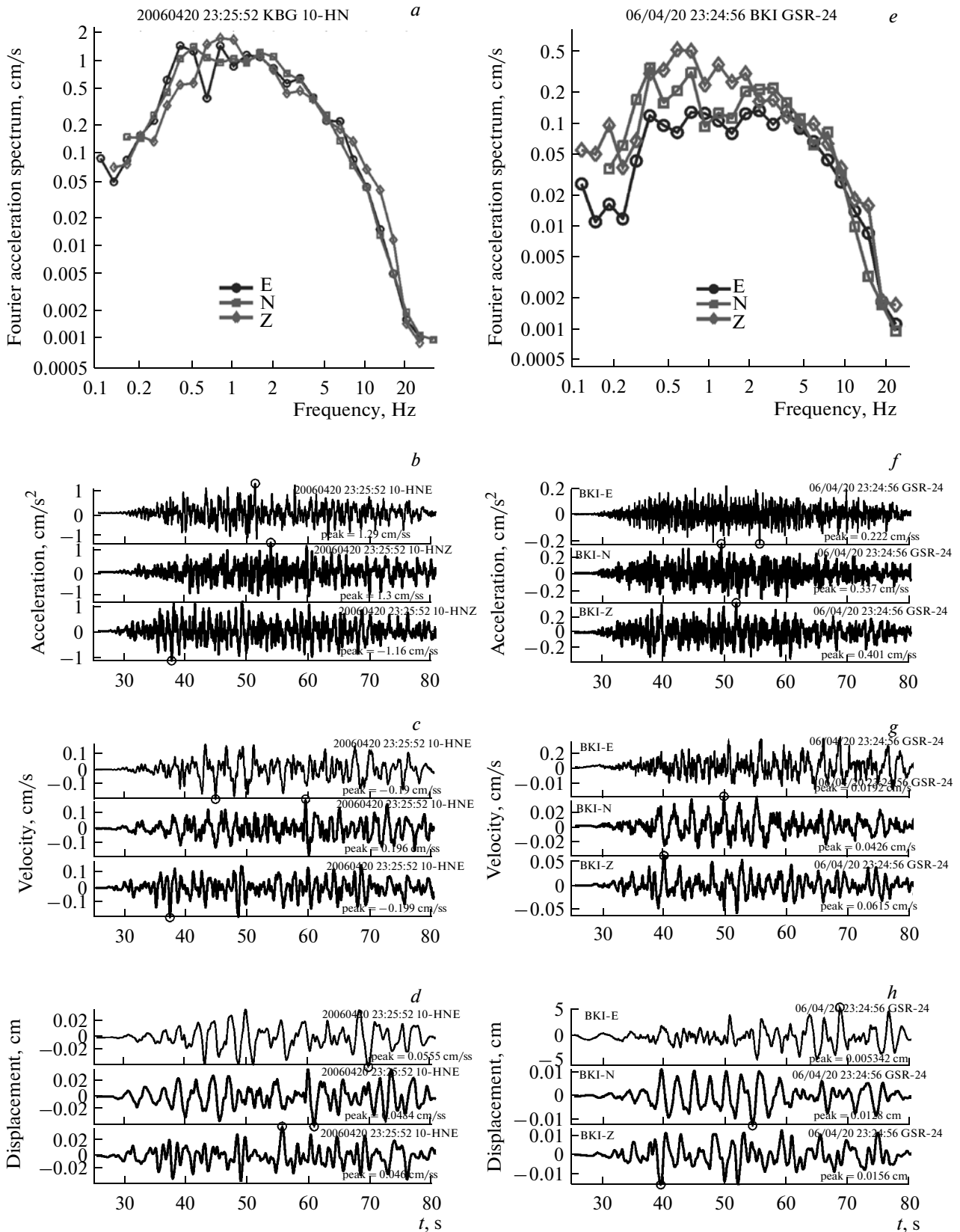
Fig. 3. Records and spectra of the P wave due to the April 20, 2006 main event as recorded at KBG and BKI: (*a*) Fourier spectra of P waves, (*b–d*) (recovered) ground motion acceleration, velocity, and displacement at KBG, (*e–h*) analogous plots for BKI.
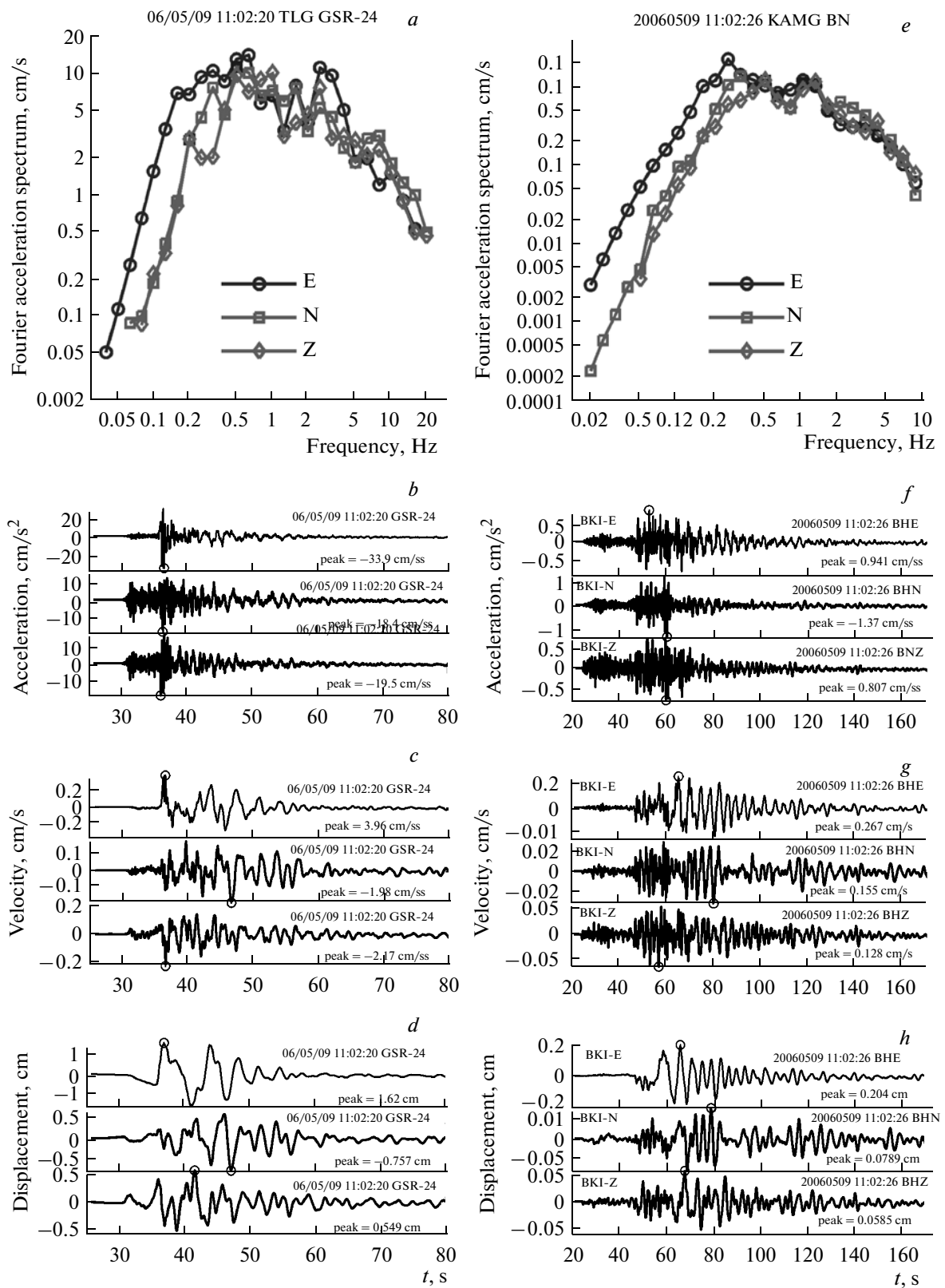
Fig. 4. Records and spectra of full records for the 11:02 May 9, 2006 aftershock ($M_L = 5.75$): (*a*) Fourier spectra for TLC records, $R = 39$ km; (*b–d*) ground motion acceleration, velocity, and displacement at TLC, (*e–h*) same for KAM, $R = 188$ km, R is hypocentral distance.

where A_S is S peak amplitude as recorded by a short period seismograph, T_S is the apparent period, and $f(r)$ a calibration function, the local magnitude can be found via K_S as follows:

$$M_L = 0.5K_S + \text{const} =$$
$$\log(A_S/T_S) + 0.5 f(r) + \text{const}. \qquad (2)$$

The constant involved should be chosen to match Richter's original definition. Gusev and Mel'nikova [4] derived a nonlinear relation of $K_{S1,2}^{F68}$ – to M_W, as well as noting a nonlinear relationship between Richter's M_L and M_W. Eliminating M_W as a parameter from these two nonlinear functions, we obtain an equation that is very similar to the following linear relation:

$$M_L = 0.5K_S - 0.75. \qquad (3)$$

The above equation has been recommended for use in magnitude conversion. We note in passing that, in the conditions of Kamchatka, teleseismic short period magnitudes are related to the new local magnitude M_L as follows:

$$m_{PV}^{(CKM)} = \text{MPVA(Obninsk)} = M_L - 0.12, \qquad (4)$$

$$m_b\,(\text{USGS}) = M_L - 0.30\,(m_b < 5.8). \qquad (5)$$

We also used teleseismic magnitude m_b along with the Kamchatka magnitude M_L. The ranges for original data are $M_L = 4.0$–6.4 for magnitude, $R = 34$–237 km for hypocentral distance, and $H = 0$–22 km for depth of focus.

The data were analyzed by multiple linear regression. Each amplitude observation Y (with subscript j) due to a magnitude M_j event at a distance of R_j is written in the form

$$\log Y_j = a_0 + b M_j - c \log R_j + \varepsilon_j, \qquad (6)$$

where ε_j is an unknown random error. We also assume that $\varepsilon_j \sim N(0, \sigma^2)$. Equation (6) is linear in the unknown parameters a_0, b, and c. The aggregate of these three parameters is, in the approximation we are considering, an empirical model of the amplitude–distance–magnitude relationship. The Y_j in the case under consideration are peak velocity or acceleration as recorded on vertical or horizontal instruments.

Equation (6) implies that the contribution of station geology is negligibly small or else is the same for all stations (and then it enters into the parameter a_0). Station soil corrections usually differ from station to station. In these conditions one can modify (6) by adding the additional unknowns (indicator variables) δ_k:

$$\log Y_j = a_0 + b M_j - c \log R_j + d_k \delta_{kj} + \varepsilon_j, \qquad (7)$$

where the parameters d_k are new unknown, station-specific corrections with $k = 1, 2, ..., K$ denoting the station; the "indicator" variable δ_{kj} K takes on the value 1, when the equation in question (with subscript j) involves the data from station k and the value 0 otherwise. The set of equations (7) is underdetermined; we obviate this difficulty by using one of the stations as the reference and putting $d_k \equiv 0$ for it. Writing down (6) or (7) for a sufficiently great number of observations, we get an overdetermined set of equations in the vector of unknowns $\{a_0, b, c\}$ or $a_0, b, c, d_1, d_2, ...\}$ which is solved by the least squares method (LS). The resulting LS solution is the desired Y–M–R relation.

The option (7) was the first to be examined. We used KAM as being installed on bedrock as the reference station and tried to determine the unknown vector $\{a_0, b, c, d_{TLC}\}$. The results turned out to be unacceptable. These problems were to be expected, since the mutual positions of two stations making a "network" and the aftershock distribution (Fig. 1) are such as to make the data of the two stations relevant to nonoverlapping ranges of distance, which leads to a strong interdependence between the components of the solution vector. In simple terms, it is easy to trade off an addition to the station correction d_{TLC} for a corresponding change in the attenuation parameter c without seriously endangering the fit. For this reason we had to estimate the soil effects (the value of d_{TLC}) by an independent method and then to convert the TLC amplitudes to those relevant for the KAM reference soil.

We determined d_{TLC} using seismic coda waves following T.G. Rautian's technique [9]. The basic data were smoothed Fourier spectra of the coda within a definite time window. There is a certain difficulty that arises because the coda spectra yield spectral corrections, while we need corrections for peaks in the time domain. We assumed that the spectral corrections, as found within the frequency band corresponding to the spectral maximum of a signal, are applicable to the peak amplitudes of that signal. The coda-wave method relies on the fact that coda amplitudes, when observed at sufficient delay times, are nearly independent of the hypocentral distance and are controlled by the earthquake source spectrum and station soil. We began by estimating the required minimum delay. This was found to be 120 s from the earthquake origin time for TLC and KAM. The next step was to construct Fourier spectra of coda records at these stations in the time interval of 120–180 s for six comparatively large aftershocks. Figure 5 shows the resulting plots for two earthquakes. It can be seen that the spectral level for TLC is substantially higher than that for KAM in the entire frequency range, so that it is in principle possible to estimate d_{TLC}. A more careful analysis showed that that the data could be used to estimate the ratio of earthquake spectra at the two stations only for frequencies below 2.5–3.0 Hz, while at higher frequencies the coda signal remained below the level of microseisms. For our purposes the frequency band 0.5–3.0 Hz is sufficient, because the bands of maximum velocity and acceleration spectra are 0.5–1.0 and 1.5–2.5 Hz, respectively. The numerical values of
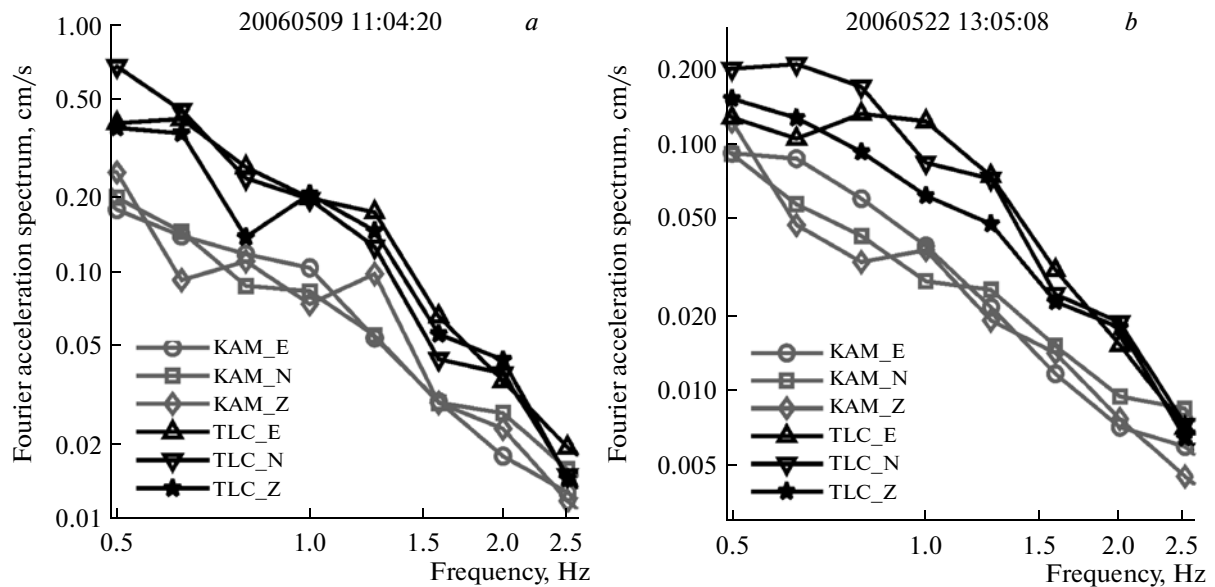
Fig. 5. Examples of smoothed Fourier acceleration spectra for coda records in the interval 120–180 s from origin time: (*a*) for the 11:02 May 9, 2006 earthquake, (*b*) for the 13:03 May 22, 2006 earthquake. Shown are the spectra of all record components at KAM and TLC.

amplitude corrections were obtained by using averaged ratios of smoothed Fourier spectra within the frequency ranges indicated above. Since we did not find any appreciable differences in the ratios of horizontal and vertical components, we averaged the ratios over all three pairs of components. The estimated soil corrections d_{TLC} are +0.29 for log acceleration (a factor of 1.95 for amplitude) and +0.38 for log velocity (a factor of 2.4 for amplitude).

These corrections were applied to observed TLC data and the regression analysis was repeated based on the following modification of (6):

$$\log Y_j = a + b(M_j - M_0) - c \log(R_j/R_0) + \varepsilon_j \quad (8)$$

with a different free term. We assumed $R_0 = 25$ km and $M_0 = 5$. The M_L and m_b magnitudes were used, while Y was represented by peak acceleration and peak velocity on vertical and horizontal components. Two processing options were carried out for the horizontal components, viz., either by using the greater of two values for a component or by analyzing all 98 equations. The regression analysis yielded very acceptable results. The parameters in (8) are listed in Table 3 for 10 processing options. The unusually large difference for the two options applied to the horizontal channels is due to the fact that the E–W amplitude was substantially greater than the N–S amplitude in an overwhelming majority of the cases. We have not been able to account for this anomaly. We recall at this point that the data in Table 3 model the amplitude attenuation for the particular soil conditions at KAM. Conversion to the TLC soil is effected by multiplying the accelerations by 1.95 and the velocities by 2.4. Brackets enclose unreliable estimates, which may have been

distorted due to a narrower recording bandwidth of the BH* channels.

The results of multiple regression analysis are preferably presented as plots, but this is difficult to do in a straightforward manner. We proceeded by calculating converted values of Y as follows:

$$\log Y_j^{(R)} = \log Y_j + c \log(R/R_0), \quad (9)$$

$$\log Y_j^{(M)} = \log Y_j b(M - M_0). \quad (10)$$

Figure 6 shows plots of converted peak acceleration (Figs. 6a–6d) and peak velocity (Figs. 6e–6h) against magnitude (Figs. 6a, 6c, 6e, and 6g) and distance (Figs. 6b, 6f, 6h). We show the equations for the larger of the two horizontal components (Figs. 6a, 6b, 6e, 6f) and for the vertical component (Figs. 6c, 6d, 6g, 6h). The effects of the corrections as applied to the TLC data are demonstarted by plotting these in two variants, with corrections (filled triangles) and without (grey triangles). Circles denote the KAM data; the soil beneath that station being adopted as the reference. The plots showing converted amplitude vs. distance (Figs. 6b, 6d, 6d, 6g) clearly demonstrate the data distribution over distance to be both very nonuniform and inhomogeneous. In the first place, there is a well-pronounced deficit of data in the distance range 60–130 km. Secondly, all data at shorter distances were recorded at TLC and nearly all data at larger distances at KAM. As a result, strong sensitivity of regression results in the variant (6) to the degree of soil homogeneity beneath the stations occurs. Meaningful results should necessarily involve station corrections, which has been done above with the additional information

Table 3. Results of regression analysis for data converted to conform to KAM site conditions

M	A/V	H/Z	a	b	c	σ	$Y(5, 25)$ "KAM"	$Y(5, 100)$ "KAM"	$Y(5, 25)$ "TLC"
M_L	A	$H(1)$	0.965	0.789	[1.825]	0.25	9.2	[0.73]	18
M_L	A	$H(2)$	0.795	0.798	[1.687]	0.25	6.2	[0.60]	12.2
M_L	A	Z	0.647	0.760	[1.652]	0.26	4.4	[0.44]	8.7
M_L	V	$H(1)$	−0.429	0.959	1.156	0.22	0.37	0.075	0.89
M_L	V	$H(2)$	−0.288	0.971	1.261	0.21	0.51	0.089	1.23
M_L	V	Z	−0.538	0.933	1.252	0.22	0.28	0.051	0.69
m_b	A	$H(1)$	0.929	0.943	[1.920]	0.27	8.4	[0.59]	17
m_b	A	Z	0.629	0.924	[1.746]	0.28	4.2	[0.37]	8.3
m_b	V	$H(1)$	−0.315	1.161	1.377	0.26	0.48	0.071	1.16
m_b	V	Z	−0.561	1.151	1.371	0.23	0.27	0.041	0.65

Note: M is magnitude type, A/V is signal type (acceleration or velocity), H/Z is the component concerned, viz., $H(1)$ is the larger of the two horizontal components, $H(2)$ is any of the two horizontal components, Z the vertical component; a, b, c, σ are parameters in (8); $Y(5, 25)$ is amplitude for $M = 5$, $R = 25$; $Y(5, 100)$ same for $R = 100$ km; "KAM" indicates quantities for KAM soil conditions, "TLC" same for TLC conditions. Square brackets enclose doubtful figures (see text).

used. The data scatter about the fitting plane (8) is given by the value $\sigma = 0.25-0.26$ log units for acceleration and $\sigma = 0.21-0.22$ log units for converted velocity. These values are quite typical of such studies in comparatively homogeneous conditions.

The resulting regressions fit our numerical data quite satisfactorily. However, there is good reason to suspect that the KAM accelerations are unreliable, because the instrumentation at that station with a digitization interval of 0.05 s and a working upper frequency of the reproducible range about 6−7 Hz is unable to faithfully record soil acceleration whose spectrum involves frequencies as high as 10−15 Hz or still higher. A crude estimate makes one expect an underestimation of acceleration amplitudes by factors of 1.2−1.8. This difficulty is also present for the velocity, but in actual practice the velocity spectrum decays rapidly above 2−3 Hz and the distortion can be disregarded. Since the contribution of KAM data at shorter distances into the level of regression curves is relatively low, the value $R = R_0 = 25$ km was chosen as the reference. As a result, the estimates of the parameter a in (3) are relatively reliable, while c for acceleration is likely to be overestimated.

DISCUSSION

We shall discuss the results of regression analysis as presented in Table 3 in conjunction with similar results for other regions. The acceleration value in column $Y(5, 25)$ coming from the processing option H1 (the greater of two peaks) is 18 cm/s² for the TLC soil conditions. These conditions can be taken as the intermediate soil type. There are estimates in the literature for mean horizontal peak acceleration and velocity for comparable magnitudes $M_L = 5$, or $M_W = 5$, or $M_S = 4.4$, or $M_{JMA} = 4.6$ at a distance of 25 km. The velocity values were for intermediate soils, while the values of acceleration were given without further bedrock−intermediate soil classification. The acceleration estimates are as follows:

71 cm/s² for Kamchatka after [12];

39 cm/s² for Japan after [11];

69 cm/s² for Japan after [14];

21 cm/s² for Greece after [15];

57 cm/s² for California after [13].

The above comparison reveals that the accelerations due to the Olyutorskii earthquake aftershocks are uncommonly low.

As to the velocities, the data given in Table 3 are paradoxical, in that the estimate for the greater horizontal component (H1) is below that for an arbitrary component (H2), thus indicating that the regression results have limited accuracy. We shall use the mean of the two estimates given above, which is close to 1.1 cm/s². The estimates for the other regions are as follows:

2.4 cm/s for California after [13];

1.4 cm/s for Greece (0.7 cm/s for bedrock with the x2 correction) after [15];

2.2 cm/s for Japan after [14].

Fig. 6. Converted ground motion amplitudes as a function of magnitude (conversion to distance $R_0 = 25$ km), (*a, c, e, g*); and as a function of distance (conversion to magnitude $M_{L0} = 5.0$), (*b, d, f, h*). (*a, b*) peak horizontal acceleration, (*c, d*) same, vertical; (*e, f*) peak horizontal velocity, (*g, h*) same, vertical. (*1*) TLC data without station correction, (*2*) same, with station correction, (*3*) KAM data, (*4*) regression lines.
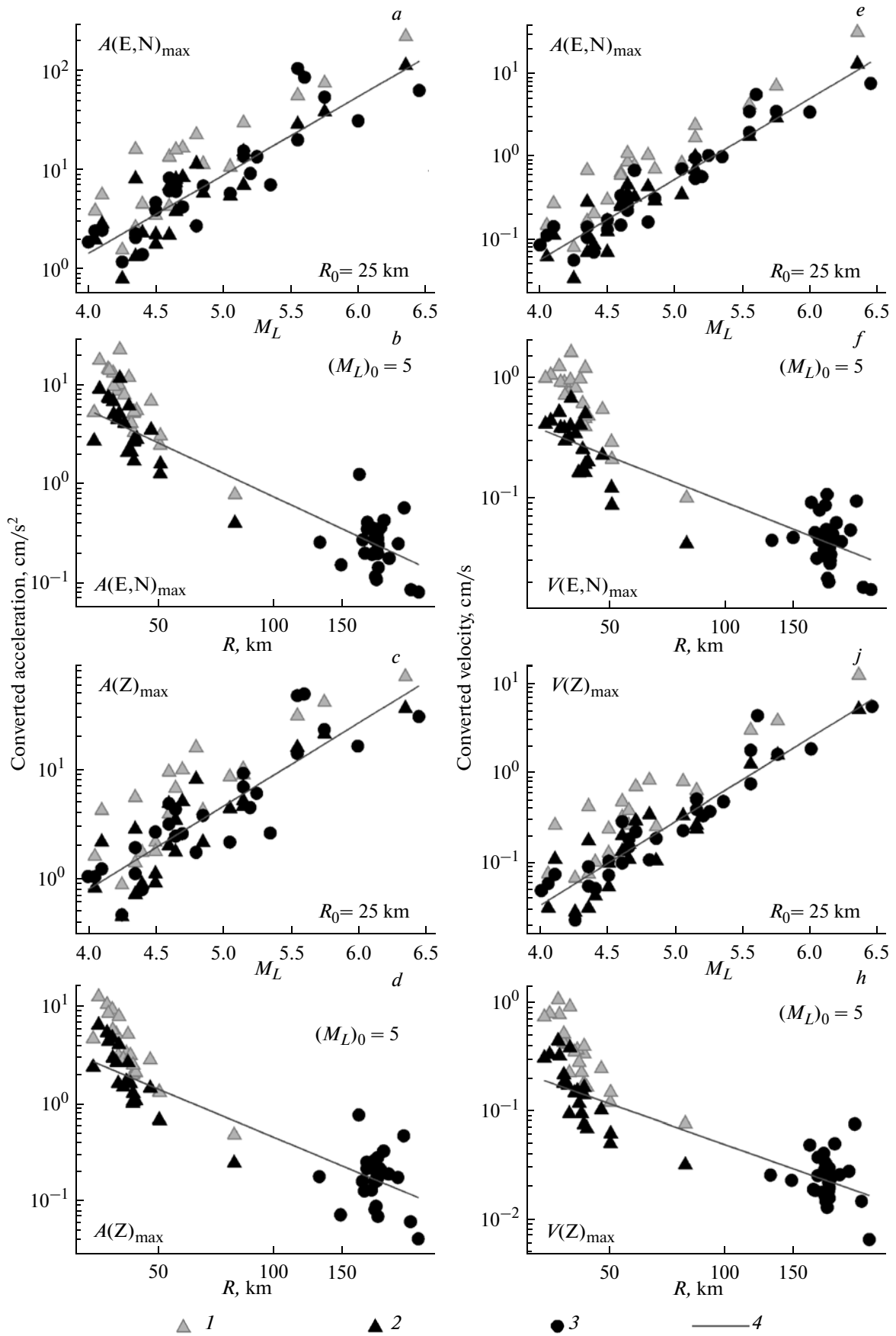
The estimates for Koryakia again turn out to be below those for the other regions. This feature for Koryakia is consistent with the fact that the frequencies of Fourier spectral peaks for velocity and (especially) acceleration are somewhat displaced toward lower frequencies relative to the mean Kamchatka spectra for M = 5–6, as could be expected in accordance with [5, 7], and this is observed at TLC, as well as at KAM. One probable cause of this anomaly is the low stress drop values for the aftershocks. It would be reasonable in the future to investigate the stress drop parameter for the records studied here. As well, it is of great interest to reconstruct the mainshock spectrum.

CONCLUSIONS

The experience of digital recording of ground motion due to the 2006 Olyutorskii earthquake and its aftershocks inspires some hope. In spite of the sparse network and certain drawbacks, valuable, although incomplete, data were acquired bearing on the main shock, in addition to some material on the aftershocks. We have inferred the mean relation of peak acceleration and velocity versus magnitude and distance for 49 aftershock records. We have detected some important features of ground motion in the little-known area of Koryakia, such as the displacement of the acceleration spectrum toward lower frequencies and the occurrence of uncommonly low (for fixed distance and magnitude) peak accelerations. The Fourier spectra of coda waves were compared to derive station corrections for the TLC station as reflecting the geology beneath that station. A basis has thus been built for obtaining quantitative estimates of the earthquake threat to buildings and structures in Koryakia using the region's own data.

ACKNOWLEDGEMENTS

REFERENCES

1. Brillinger, D.R., *Time Series. Data Analysis and Theory*, New York–Chicago: Holt, Rinehart and Winston, Inc., 1975.

2. Gusev, A.A. and Guseva, E.M., Ground Motion Due to Large Earthquakes in Kamchatka: A Review, *Vulkanol. Seismol.*, 2006, no. 4, pp. 14–24.

3. Guseva, E.M., Gusev, A.A., and Oskorbin, L.S., A Program Package for Digital Processing of Seismic Records and Its Application to Some Sample Records of Strong Ground Motion, *Vulkanol. Seismol.*, 1989, no. 5, pp. 35–49.

4. Gusev, A.A. and Mel'nikova, V.N., Magnitude Relationships: Worldwide and for Kamchatka, *Vulkanol. Seismol.*, 1990, no. 6, pp.55–63.

5. Gusev, A.A., Petukhin, A.G., Guseva, E.M., et al., Average Fourier Spectra of Strong Ground Motion Due to Kamchatka Earthquakes, *Vulkanol. Seismol.*, 2006, no. 5, pp. 60–70.

6. Gusev, A.A., Chubarova, O.S., Chebrov, V.N., and Abubakirov, I.R., Ground Motion Due to the April 20(21), 2006 Olyutorskii Earthquake and Its Aftershocks Inferred from Digital Records: Preliminary Results, in *Olyutorskoe zemletryasenie (20(21) aprelya 2006 g., Koryakskoe nagor'e). Pervye rezul'taty issledovanii* (The April 20(21), 2006 Olyutorskii Earthquake, Koryak Upland: First Results), Petropavlovsk-Kamchatskii: GS RAN, 2007, pp. 263–276.

7. Gusev, A.A., Shumilina, L.S., and Akatova, K.N., On the Assessment of Earthquake Hazard for the Town of Petropavlovsk-Kamchatskii Based on a Set of Scenario Earthquakes, *Vestnik Otdeleniya Nauk o Zemle. Elektronnyi Nauchno-Informatsionnyi Zhurnal*, 2005, no. 1(23): URL: http://www.scgis.ru/Russian/cp1251/h_dgggms/1-2005/screp-2.pdf.

8. Kuzin, I.P., *Fokal'naya zona i stroenie verkhnei mantii v raione Vostochnoi Kamchatki* (The Benioff Zone and Upper Mantle Structure beneath Eastern Kamchatka), Moscow: Nauka, 1974.

9. Rautian, T.G., Khalturin, V.I., Zakirov, M.S., et al., *Eksperimental'nye issledovaniya seismicheskoi kody* (Experimental Studies of the Seismic Coda), Moscow: Nauka, 1981.

10. Fedotov, S.A. *Energeticheskaya klassifikatsiya Kurilo-Kamchatskikh zemletryasenii i problema magnitud* (The Energy Classification of Earthquakes and the Magnitude Problem), Moscow: Nauka, 1972.

11. Fukushima, Y. and Tanaka, T., A New Attenuation Relation for Peak Horizontal Acceleration of Strong Earthquake Ground Motion in Japan, *Bull. Seismol. Soc. Amer.*, 1991, vol. 80, pp. 757–783.

12. Gusev, A.A., Gordeev, E.I., Guseva, E.M. et al., The First Version of the $A_{max}(M_W, R)$ Relationship for Kamchatka, *PAGEOPH*, 1997, vol. 149, pp. 299–312.

13. Joyner, W.B. and Boore, D.M., *Estimation of Response-Spectral Values as Functions of Magnitude, Distance and Site Conditions*, USGS Open-File Report 82-881, 1982.

14. Kawashima, K., Aizawa, K, and Takahashi, K., Attenuation of Peak Ground Acceleration, Velocity and Displacement Based on Multiple Regression Analysis of Japanese Strong Motion Records, *Earthquake Engineering and Structural Dynamics*, 1986, vol. 14, pp. 199–215.

15. Theodulidis, N. and Papazachos, B., Dependence of Strong Ground Motion on Magnitude, Distance, Site Geology and Macroseismic Intensity for Shallow Earthquakes in Greece, *Soil Dynamics and Earthq. Eng.,* 1992, vol. 13, pp. 317–343.

SPELL: OK